Submission type: Article | Discoveries

Genetic mapping reveals an anthocyanin biosynthesis pathway gene potentially influencing evolutionary divergence between two subspecies of scarlet gilia (*Ipomopsis aggregata*)

Brandon E. Campitelli[1], Amanda M. Kenney[1,2], Robin Hopkins[1,3], Jacob Soule[1], John T. Lovell[1,4], Thomas E. Juenger[1]

[1]The University of Texas at Austin, Department of Integrative Biology, 2415 Speedway C093, Austin, Texas, 78712

[2] Current address: Biotechnology Risk Analysis Programs, USDA-APHIS-BRS, 4700 River Road, Riverdale, MD, 20737

[3]Current address: Harvard University, Department of Organismic and Evolution Biology, Arnold Arboretum, 1300 Centre Street, Boston, MA 02131

[4]Current address: Hudson Alpha Institute for Biotechnology, Huntsville, AL, USA 35806

Corresponding authors: BEC, TEJ
E-mail: brandon.campitelli@gmail.com, tjuenger@austin.utexas.edu

ABSTRACT

Immense floral trait variation has likely arisen as an adaptation to attract pollinators. Different pollinator syndromes—suites of floral traits that attract specific pollinator functional groups—are repeatedly observed across closely related taxa or divergent populations. The observation of these trait syndromes suggests that pollinators use floral cues to signal the underlying nectar reward, and that complex trait combinations may persist and evolve through genetic correlations. Here, we explore pollinator preferences and the genetic architecture of floral divergence using an extensive genetic mapping study in the hybrid zone of two *Ipomopsis aggregata* subspecies that exhibit a hummingbird and a hawkmoth pollinator syndrome. We found that natural selection acts on several floral traits, and that hummingbirds and hawkmoths exhibited flower color preferences as predicted by their respective pollinator syndromes. Our quantitative trait loci (QTL) analyses revealed 46 loci affecting floral features, many of which co-localize across the genome. Two of these QTL have large effects explaining > 15 percent of the phenotypic variance. The strongest QTL was associated with flower color and localized to a SNP in the anthocyanin biosynthesis pathway (ABP) gene, *dihydroflavonol-4-reductase* (*DFR*). Further analysis revealed strong associations between *DFR* SNP variants, gene expression and flower color across populations from the hybrid zone. Hence, *DFR* may be a target of pollinator-mediated selection in the hybrid zone of these two subspecies. Together, our findings suggest that hummingbirds and hawkmoths exhibit contrasting flower color preferences, which may drive the divergence of several floral traits through correlated trait evolution.

INTRODUCTION

Flowers are one of the most diverse group of plant organs, exhibiting immense inter- and intra-specific variation in shape, size, color, scent, and reward. Given the direct link between flowers and plant reproduction, it is commonly hypothesized that these traits respond to persistent and strong pollinator-mediated natural selection, which results in fine-tuned adaptation to attract effective pollinators (Baker and Hurd 1968; Stebbins 1970a; Campbell 1996). Variable pollinator preferences can cause floral trait divergence between plant populations through pollinator-mediated selection (Grant 1949), especially when populations occur in allopatry. For example, suites of floral traits may adapt to the most prevalent and/or efficient pollinators, and subsequent pollinator preference may reinforce population divergence by limiting intercrossing and gene flow upon secondary contact (Grant 1949).

Suites of traits that attract specific groups of pollinators—so called pollination syndromes—have evolved repeatedly among flowering plants (Grant 1949; Baker 1963; Stebbins 1970b; Proctor et al. 1996; Hermann and Kuhlemeier 2011), supporting a role for pollinator preference as a driver of floral divergence. However, the emergence of pollinator syndromes necessarily requires coordinated evolutionary changes across multiple complex traits. Hence, while pollinator preferences may provide a source of divergent selection acting on floral trait variation, other factors are likely to play important roles in the evolution of floral divergence. For example, both pleiotropy — where a single gene affects multiple traits — and genetic linkage between multiple genes can cause genetic correlations of floral traits. Genetic correlations are expected to affect the response to selection, and hence the rate of evolutionary divergence between suites of traits (Smith et al. 1985; Mitchell-Olds 1996; Conner 2002; Smith 2016). For example, multivariate evolutionary responses to selection will be strengthened if the direction of selection matches the axis of maximum genetic correlations among traits (Etterson and Shaw 2001; Brock et al. 2010; Lovell et al. 2013). This process could accelerate floral divergence between populations with pollinator communities that possess contrasting preferences that align with these correlated traits. Alternatively, if pollinator-mediated selection favors increases (or decreases) in traits that are negatively genetically correlated (*i.e.*, antagonistic pleiotropy), this could constrain the evolutionary response of these traits (Etterson and Shaw 2001; Brock et al. 2010; Lovell et al. 2013), and limit the potential for populations to diverge and coevolve with novel pollinators. Thus, knowledge of the genetic basis of floral diversity may help to elucidate the potential for adaptation to changes in pollinator communities.

One of the best studied traits between florally diverged groups is flower color. Natural flower color variation typically arises from polymorphisms within the anthocyanin biosynthetic pathway (ABP, see Fig. S1 for a schematic; adapted from Zufall and Rausher 2004). The ABP is a well-characterized and highly-conserved pathway responsible for the production of anthocyanin flavonoids that are involved in a variety of plant functions, including floral color pigmentation (Forkmann 1991; Holton and Cornish 1995). Regulatory changes of—or mutations directly to—genes within the ABP, often lead to altered or loss of function of key pathway

enzymes that are required to convert anthocyanin precursors into pigments (Whittall et al. 2006; Rausher 2008; Smith and Rausher 2011), which alters flower color and could result in a shift of pollinator preferences and community. For example, gene inactivation of *anthocyanin2* (a regulatory gene of the ABP) reduces pink floral pigmentation in several *Petunia* accessions; evidence from transgenic experiments suggests that lines with contrasting *an2* alleles attract different pollinators (Quattrocchio et al. 1999; Hoballah et al. 2007). Floral transitions from colored to non-colored flowers are likely to occur through a loss/reduction of function of an enzyme or regulatory element required for pigment production, which can subsequently lead to a shift in their primary pollinator community (Rausher 2008; Smith and Rausher 2011; Wessinger and Rausher 2015).

Recent advancements in genetic marker development have led to an increase in studies that have explored the genetic architecture of floral divergence. Specifically, in the last two decades, quantitative trait loci (QTL) mapping studies conducted on intercrosses between sister-taxa or subspecies pairs with different pollination syndromes have been enormously valuable for elucidating genetic architecture and have revealed some common underlying patterns (reviewed by Hermann and Kuhlemeier 2011). For example, flower color and nectar variation are often characterized by a few large effect QTL (*e.g.*, Nakazato et al. 2013), whereas QTL affecting morphological variation (*i.e.*, flower shape and size) are typically more numerous and of minor effect sizes (*e.g.*, Juenger et al. 2000; Fishman et al. 2002; Juenger et al. 2005; Fishman et al. 2015). Importantly, in many cases there is evidence that QTL for different traits co-localize in the genome (Juenger et al. 2000; Conner 2002; Juenger, Perez-Perez, et al. 2005; Ashman and Majetic 2006), further suggesting that display and reward traits may have been evolutionarily "packaged" together and underlie common pollinator syndromes. While these studies have enhanced our understanding of the interplay between pollinator-mediated selection and the genetic architecture of floral divergence across a number of species, few have simultaneously evaluated the genetic architecture of floral divergence and pollinator behavior together (see Schemske and Bradshaw 1999; Bradshaw and Schemske 2003).

A number of research groups have explored the underlying molecular genetics of floral traits in several ecological model systems: for example, *Mimulus* (Macnair and Cumbes 1989; Lin and Ritland 1997; Bradshaw and Schemske 2003), *Aquilegia* (Fulton and Hodges 1999; Hodges et al. 2002), *Ipomoea* (Paulsen and Rausher 2000; Subramaniam and Rausher 2000; Zufall and Rausher 2004; Des Marais and Rausher 2010), and *Phlox* (Hopkins and Rausher 2011; Hopkins and Rausher 2012). Furthermore, there are a growing number of examples of identifying genes that underlie florally diverged traits (*e.g.*, Hoballah et al. 2007; Hopkins and Rausher 2011; Yuan et al. 2013; Amrad et al. 2016). In the current study, we present data from two experiments that together examine the interplay of pollinator-mediated selection and genetic architecture, in combination with the molecular genetics of candidate flower color genes, to better understand floral divergence between two closely related subspecies of *Ipomopsis aggregata*.

The *I. aggregata* (Polemoniaceae) species complex contains at least eight known subspecies that collectively inhabit most of the western United States, with several contact zones where hybrids are frequently reported (Wilken and Allard 1986; Wolf et al. 1991; Wolf and Soltis 1992; Porter and Johnson 2000; Porter et al. 2010). There has been a long and rich history of study of the *I. aggregata* species complex that has focused on co-evolutionary interactions with pollinators (hummingbirds, hawkmoths, bees, butterflies), and has revealed an important role for pollinator dynamics in hybridization and diversification among subspecies (Grant 1992). For example, long-term and detailed field studies carried out on *I. aggregata* subspecies *aggregata* have discovered that variation in pollinator visitation and efficiency can impose strong natural selection on many floral characters. These include, for example, flower size and shape (Campbell 1989; Campbell 1991; Campbell 1996), inflorescence display (Campbell 1991; Mitchell 1994; Juenger, Morton, et al. 2005), nectar production (Mitchell and Waser 1992; Mitchell 1993), the coordinated phenology of male and female reproduction (Campbell 1991; Campbell 1997; Campbell et al. 1997), and that pollinator-mediated selection pressures on floral morphology can vary between hummingbirds and hawkmoths (Campbell 1997; Melendez-Ackerman 1997; Melendez-Ackerman and Campbell 1998; Campbell 2003). Given the extensive evidence of natural selection on many reproductive traits, the *I. aggregata* complex offers an ideal system to explore the interplay of genetic architecture and pollinator preferences on floral divergence.

In previous work (Milano et al. 2016), we studied patterns of floral trait divergence between the subspecies pair of *I. aggregata*, *I. aggregata* subsp. *candida* (Rydb.) V.E. & A.D. Grant, and *I. aggregata* subsp. *collina* (Greene) Wilken & Allard. We hereafter refer to these as *candida* and *collina* (Grant and Wilken 1987). *Candida* flowers are thin and long, have inserted anthers, sparse nectar production, and range in color from pure white to pale pink, which is typical of a hawkmoth pollinator syndrome (Fig. 1A). *Collina* flowers are shorter and wider than *candida*, have exerted anthers, produce copious dilute nectar, and are red, which are characteristics common to a hummingbird pollinator syndrome (Fig. 1A). Phylogenetic analyses suggest that the *collina*-type represents the ancestral condition (Porter and Johnson 2000; Porter et al. 2010). Grant and Wilken (1987) proposed that the *candida* morph diverged allopatrically from a *collina*-like ancestor during the last glacial maximum, followed by secondary contact between *collina* and *candida* after glacial retreat. Wolf et al. (1991) suggested an alternative evolutionary history that the two subspecies are undergoing primary divergence. In our previous work, we discovered significant quantitative genetic differentiation for several floral features, including corolla width, corolla length, flower color, and nectar volume, across a representative collection of 27 populations that cover the hybrid zone in the Colorado Rockies (Milano et al. 2016), despite abundant gene flow between sites (Milano et al. 2016). While these results indicate that there has likely been persistent divergent selection capable of withstanding the homogenizing effects of pervasive gene flow, it is unclear whether pollinator-mediated selection and/or genetic architecture contribute to this floral divergence.

Here, we build on previous work by exploring the fitness effects of floral traits that exhibit strong population divergence and assess natural pollinator preferences in the field using a large QTL mapping population generated from a cross between *candida* and *collina*. In the same field experiment, we characterize the genetic architecture of divergent floral traits using a QTL mapping study. Finally, we investigate the genetic basis of flower color divergence by quantifying gene expression variation of several candidate genes in the ABP from individuals collected across Colorado's Front Range. Specifically, our study addresses the following major questions: (1) What traits contribute to overall plant fitness in the field, and do we observe pollinator preferences for floral traits? (2) What is the underlying genetic architecture of floral divergence, and can this inform our understanding of the processes that drove divergence? (3) Is there evidence that genetic variation or regulatory changes in candidate ABP genes affect flower color variation?

RESULTS

Natural selection on floral features, and pollinator preferences

To better understand the drivers of evolutionary divergence between *candida* and *collina*, we first planted an outbred F_2 mapping population (see Materials and Methods and Fig. 1A to C for a detailed crossing design) into an experimental garden located in the Front Range of the Colorado Rocky Mountains. We then measured 18 traits including phenotypes previously shown to be genetically differentiated between natural populations (Milano et al. 2016). We scored the following traits: flowering time, seven floral morphology traits (Fig. 1D), four plant size traits (number of flowers, number of inflorescence branches, height, and the diameter of the root stock at soil level), flower color, nectar volume and concentration, pollinator visitation rates by hummingbirds (HBird) and hawkmoths (HMoth), and fitness as a relativized fruit count. Full trait descriptions are provided in the Materials and Methods section. Raw phenotypic correlations ranged from weak (Pearson's $r = 0.01$) to relatively strong (Pearson's $r = 0.68$; Fig. S2A), with many of the stronger correlations occurring among floral morphology traits (purple box in Fig. S2A) and plant size traits (purple box in Fig. S2A). Hence, to reduce dimensionality for our selection analysis we used PCAs to collapse floral morphology traits into PCFsize (PC1, 55.6% variation explained, small to large) and PCFshape (PC2, 15.6% variation explained, wide to long; Fig. S3A), and plant size traits into PCsize (PC1, 52.3% variation explained; Fig. S3B).

Our goals were to first estimate phenotypic selection acting on both traits and pollinator visitation in the field, and then explore how the traits influenced pollinator visitation. To this end, we utilized a series of generalized linear models to (a) determine the effects of each phenotype on fitness, (b) the effect of pollinator visitation on fitness, and (c) the effects of each phenotype on hummingbird and hawkmoth visitation. Our first selection analysis revealed that larger and earlier flowering plants, with larger flowers and increased nectar volume had greater relative fitness (MODEL 1 in Fig. 2A). Higher rates of visitation by either pollinator also led to increased fitness (MODEL 2 in Fig. 2A). Our pollinator-specific models indicate that greater nectar

production resulted increased visitation rates from both pollinators (MODELs 3 & 4 in Fig. 2B). In addition, hummingbirds showed a preference for visiting larger plants (MODEL 3 in Fig. 2B). As predicted, we found divergent preferences for flower color; hummingbirds preferentially visited red flowers (indicated by the dashed line in Fig. 2B), whereas hawkmoths preferentially visited white/pale pink flowers (indicated by the solid line in Fig. 2B). These divergent preferences can be clearly seen in surface plots constructed from predicted visitation values estimated using MODELs 3 & 4 (Fig. 2C). In addition to our linear results above, we discovered a nonlinear pattern of selection on PCFshape (Fig. 2A, Table S1), and inspection of a partial regression plot (Fig. S4A) shows a weak disruptive pattern, suggesting selection acting against intermediate shaped flowers (*i.e.*, neither wide nor long). Furthermore, the following traits showed weak nonlinear effects on hummingbird visitation only (Fig. 2B, Table S1), with curvature determined by partial regression plots (Fig. S4B-D): Flowering time showed a stabilizing pattern, PCFsize showed a disruptive pattern, and PCsize showed an increasingly positive pattern with no minima or maxima.

Genetic architecture and QTL mapping analysis

Our outbred F2 mapping population was derived by intercrossing two separate *candida* × *collina* F_1 hybrids (families, Fig. 1). As an initial scan of genetic architecture, we inspected the distribution of trait values across all F_2 individuals as well as split by family. The impact of family was moderate in most phenotypes, as evidenced by approximately normal distributions in most traits. However, flowering time and flower color exhibited strong bimodal distributions. Interestingly, the bimodality of flowering time and color appears to be driven by variation within the two different families, where family 1 had a bimodal flower color distribution, and family 2 had a bimodal flowering time distribution (as can be seen by the spread of red and blue dots in Fig. S2B for these two traits). This pattern is typically indicative of the segregation of one or a few large effect loci for these traits in only one, but not both, families.

To explore the genetic basis of these patterns of phenotypic variation we conducted QTL mapping. We genotyped the F_2 mapping population at 55 genetic markers (42 microsatellites and 13 expressed sequence tag single nucleotide polymorphisms, EST-SNPs; Table S2), and constructed a linkage map for QTL mapping (described fully in the Materials and Methods section). Several EST-SNPs were located within known ABP genes and identified in EST sequencing of floral and leaf tissue collected from several *candida* and *collina* populations. These included *chalcone synthase* (*CHS*), *flavanone-3-hydroxylase* (*F3H*), *dihydroflavonol 4-reductase* (*DFR*), and *anthocyanidin synthase* (*ANS*) (Fig. S1); these structural ABP genes have previously been implicated in flower color variation (Zufall and Rausher 2004; Whittall et al. 2006). We used genomewide QTL scans to identify genomic regions affecting the floral, growth, and visitation phenotypes collected in the field (Fig. 3). In total, when including PC traits, we discovered 46 QTL that explained variation in 17 of 21 traits (Fig. 3, Table S3 provides a summary of all QTL); we did not detect any significant QTL for nectar concentration, hawkmoth visitation, PCsize, or number of branches.

The majority of phenotypically correlated characters possessed multiple overlapping QTL across the genome, suggesting that in many cases these phenotypic correlations are reflective of underlying genetic correlations resulting from physical linkage or pleiotropy. However, several strongly correlated phenotypes (*e.g.*, plant height and number of flowers, or corolla tube length and stamen filament length; Fig S2A) did not share overlapping QTL, suggesting that these traits are either environmentally correlated and/or there is considerable epistasis and/or there are small effect pleiotropic or genetically linked loci that we did not detect.

We mapped a single QTL for relative fitness, root diameter, and number of flowers, while all remaining traits had multiple QTL. Two of the QTL we detected had relatively large additive effects; one for flower color located on LG1 (Col_1_61.2) had 35.8 PVE (percent variance explained) for flower color, and one for flowering time on LG7 had 15.7 PVE (FT_7_64; Fig. 4A, Table S3). These two large effect QTL may help explain the bimodal distributions we detected for flower color and flowering time. The remaining QTL explained relatively less of the variance (PVE <16%; Table S3), suggesting that most traits are governed by many smaller effect loci. With the exception of hummingbird visitation, relative fitness, and size traits, the QTL we detected cumulatively explained >16% of the variance for each trait (Table S3).

QTL Col_1_61.2 maps to a marker in *DFR*. This is a large effect QTL for both flower color and hummingbird visitation and is the largest LOD peak (not significant, LOD = 3.26, p = 0.52) detected for hawkmoth visitation. We found that hummingbird visitation increased with alleles inherited from *collina*-like grandparents (Fig. 4B), and hawkmoth visitation increased with alleles inherited from *candida*-like grandparents (Fig. 4C). These data support our finding of pollinator preferences for divergent flower colors, and suggest that *DFR*—or a linked locus—may be important for response to pollinator-mediated selection.

F3H is located on LG2 and co-localized with QTL for petal width, corolla tube width, PCFsize, and HBird, while *CHS* is located on LG3 and co-localized with corolla tube width (Fig. 3). *ANS* was also located on LG3, but did not co-localize with any traits considered here. These results suggest that variation in *F3H* and *CHS* may be genetically linked to loci that affect floral morphology and potentially hummingbird visitation.

We discovered that both family and maternal cytoplasm (see Fig. 1C) had moderate additive effects on our power to detect some QTL and that QTL effects were often dependent on family (see Fig. S5). For especially large family effects, this suggests that at least one F1 parent was likely homozygous at a QTL affecting these traits. This is again consistent with the bimodal distributions we observed for flowering time and color, and effect plots for these two traits in particular reveal strong family differences (Fig. 4D, E). For example, individuals in family 1 flowered later irrespective of their genotype at the large effect QTL on LG7; however only individuals with specific *candida* alleles (specifically the Ca_2 allele) had later flowering and

individuals with specific *collina* alleles (specifically a Co_2 allele) had earlier flowering in family 2 (Fig. 4D). The large effect flower color QTL on LG1 also shows an interesting difference between families; family 1 always expresses whiter flowers irrespective of genotype (Fig. 4E). Many other QTL also exhibited effect patterns dependent on family (Fig. S5, S6).

Generally, we found that most QTL affected phenotypic variation in the expected direction based on evolutionary divergences observed between *candida* and *collina* subspecies (effect plots in Fig. S6). For example, alleles inherited from a *collina*-like grandparent generally led to individuals with redder flowers (Fig. S6D, E), higher nectar production (Fig. S6F, G), and shorter, wider corollas (Fig. S6X – AH, AK; compare the effect of Co vs. Ca alleles). Yet, some QTL showed patterns that do not match expectations based on divergence (*e.g.*, *collina* alleles leading to longer stigmas; Fig. S6AM). For most traits with multiple QTL, the allelic effects across QTL were aligned, reinforcing the phenotypic effect (for example, all of the corolla tube width QTL generally showed increased width with more Co alleles; Fig. S6X – AF), but we observed a few instances where allelic effects across QTL were in opposition (for example, stigma length shortened with Co alleles for two QTL, but lengthened with Co alleles for its third QTL; Fig. S6AL – AN).

Analysis of candidate flower color genes

Our QTL mapping from controlled crosses is a powerful tool to detect important loci but unfortunately is restricted to sampling only a handful of possible naturally segregating alleles. This limits the inference that can be made about genetic architecture of variable traits. To complement our QTL mapping results, we tested for associations between candidate gene variation and floral display traits in natural populations. To this end, we sampled 265 individuals from 15 natural populations in the Front Range hybrid zone (site summaries found in Table S4), and tested for associations between SNP variation in ABP genes, flower color, and gene expression. Our initial analysis centered on exploring the relationship between gene expression levels and color across all individuals. Because we expected strong population structure for floral traits including color (Milano et al. 2016), we included site as a random factor in our model. Any associations would be driven by either non-synonymous polymorphism at candidate loci or expression level differences between SNP variants at each locus. To explore this latter idea, we also evaluate differences between SNP variant gene expression and color for each ABP locus individually.

We discovered that *DFR* expression strongly predicts flower color among individuals across the Front Range, with higher expression being correlated with redder flowers (Fig. 5A). This relationship holds even when controlling for the strong population structure in both flower color and gene expression in our sampling, as illustrated in Fig. 5B. In addition, *DFR* SNP variants were differentially expressed ($F = 8.56$, $p = 0.004$) and exhibited dramatically different colors ($F = 8.39$, $p = 0.004$; Fig. 6), providing evidence that natural variation in *DFR* gene expression levels may affect flower color.

In contrast with our findings for *DFR*, we found no evidence that *CHS, F3H,* or *ANS* expression predicted flower color across individuals (Fig. S7). Furthermore, we see no clear patterns between mean site gene expression and flower color for these three genes (Fig. 5B), despite significant differences between sites for expression (*CHS, F* = 1.98, *p* = 0.02; *F3'H, F* = 2.23, *p* = 0.007; *ANS, F* = 3.33, *p* < 0.0001). An analysis of SNP variants at these loci yielded inconclusive patterns connecting gene expression and flower color for *F3H* and *ANS*. For example, SNP variant XX for *F3H* had lower expression than the other variants (*F* = 8.54, *p* = 0.0004), but this was not associated with a flower color change. Instead, it was SNP variant YY for *F3H* that had significantly different color (SNP variant YY; *F* = 4.00, *p* = 0.05). Similarly, although both SNP variants for *ANS* has the same expression (*F* = 0.00, *p* = 0.97), they were significantly different for flower color (*F* = 4.07, *p* = 0.04. There were no differences in expression or color among *CHS* SNP variants. Together, our molecular analysis of four ABP genes suggests an association between *DFR*—but not *CHS, F3H* or *ANS*—genetic variation, gene expression, and flower color divergence between *candida* and *collina* in the Front Range hybrid zone.

DISCUSSION

Our results revealed several major findings. First, our field experiment detected natural selection acting on several phenotypes, including two floral traits. Moreover, we found that two primary pollinators exhibited preferences for divergent flower colors in *I. aggregata*, which appears to be strongly mediated by genetic variation at a single locus. Second, a QTL analysis revealed two major effect loci, one of these—which is linked to *DFR*—affecting flower color, and several smaller effect and overlapping loci for many of the traits. These patterns suggest that pleiotropy and/or genetic linkage play an important role in trait divergence amongst pollination syndromes. In addition, most of the QTL affected phenotypic variation in the direction expected based on floral divergence, consistent with a history of divergent natural selection. Finally, a more detailed exploration reveals that genetic variation at the QTL linked to *DFR* potentially influences pollinator visitation, and that *DFR* gene expression and flower color are strongly associated across the Front Range, suggesting that *DFR*—or a closely linked gene—may be a common source of flower color variation for pollinator-mediated natural selection to act on. We elaborate on these findings below.

Natural and pollinator-mediated selection on floral features

We measured selection acting on several of the plant traits in our field experiment (Fig. 2). We found selection favoring early flowering, which is consistent with previous studies in a variety of plant systems (Austen et al. 2017), including in the *Ipomopsis aggregata* system (Campbell 1991; Juenger and Bergelson 1997; Juenger and Bergelson 2000; Freeman et al. 2003). Plant size also had a large effect on fitness; a larger PCsize score corresponded to plants that were taller, branchier, produced more flowers, and had higher fitness. We found that plant

size significantly contributed to hummingbird visitation rate indicating that larger plants with larger floral displays attracted more pollinators (Fig. 2). Since *I. aggregata* is an obligate outcrosser and is pollen limited (Juenger and Bergelson 1997), attracting more pollinators resulted in greater fruit production. In addition, we found a positive phenotypic correlation between plant size and nectar volume, selection favoring increasing nectar production, and a preference by both pollinators for individuals that produced a larger nectar reward (Fig. 2, S2). These findings suggest that greater nectar production led to greater fitness through increased pollinator visitation. Finally, we discovered weak positive selection for traits that increase overall flower size (PCFsize). We believe this was driven primarily through a strong phenotypic correlation between PCFsize and flowering time, and a potential genetic correlation supported by overlapping QTL on LGs 3 and 7, suggesting that selection acting on earlier flowering may have indirectly selected for larger flowers, or vice versa.

Hummingbirds and hawkmoths exhibit divergent preferences for flower color

We detected strong divergent pollinator preferences for color (Fig. 2B), with hummingbirds preferentially visiting red flowers and hawkmoths visiting white/pale pink flowers, confirming the findings of several previous studies (*e.g.*, Meléndez-Ackerman et al. 1997). Given the preference for high nectar volume exhibited by hawkmoths, the color preference by hawkmoths must have been relatively strong to counteract the indirect selection for red flowers due to selection on and correlation with nectar volume. It is important to note that the observed selection coefficients may be indirect. For example, the pollinators could have been searching based on a trait closely genetically linked to color that we did not measure in this study (*e.g.*, scent).

We did not detect the expected divergent pollinator visitation pattern for flower shape based on the hummingbird-hawkmoth pollinator syndrome (i.e., that hummingbirds would prefer short-wider flowers while hawkmoths would prefer long-thinner flowers) (Campbell 1997; Meléndez-Ackerman et al. 1997; Melendez-Ackerman and Campbell 1998). The lack of divergent preferences for floral morphology may have resulted from pollinators simply choosing flowers with more nectar, which shared multiple overlapping QTL with flower width traits on LG3, and hence could have conflicted with expected hawkmoth preference for narrower flowers. This suggests that pollinators were learning which flowers carried more reward during the course of the summer field season. Many other studies have demonstrated that both hummingbirds and hawkmoths are remarkably flexible in their capacity to learn (*e.g.*, Meléndez-Ackerman et al. 1997), supporting the notion that these animals may have been targeting flowers that produced copious nectar. We personally observed this, particularly with hummingbirds, in that they were clearly competing for resources by defending large and high-nectar producing individuals, irrespective of flower color, across the season. Despite no direct visitation evidence to support pollinator shape preference, we note that we did find weak disruptive selection acting on PCFshape, such that plants with wide or long flowers had marginally higher fitness than plants with intermediate-shaped flowers (Fig. S4A). This suggests either the existence of divergent

pollinator preferences that we did not have power to detect, or reduced pollinator efficacy on intermediate non-optimally shaped flowers.

The role of genetic architecture and pollinator preference on floral divergence

Our experimental approach focused on recombining parental genotypes with diverged floral traits typical of hawkmoth and hummingbird pollination syndromes. Despite experimental recombination, our hybrid progeny maintained many trait correlations (Fig. S2) and extensive clustering of QTL (Fig. 3). This suggests a prominent role for genetic correlations in structuring the divergent evolution of these traits (Lovell et al. 2013). For example, the strong preference for different flower colors exhibited by hummingbirds and hawkmoths could potentially drive divergence in flower size traits, nectar volume, and flowering time through genetic correlations. All of these traits were phenotypically correlated and shared overlapping QTL (Fig. 3, S2) confirming that they are genetically correlated, and our previous work has shown that they are differentiated across Front Range sites in this system (Milano et al. 2016). These findings reflect those of other studies that have characterized the genetic architecture of floral divergence. For example, in the closely related species pair, *I. guttata* and *I. tenuifolia*, Nakazato et al. (2013) mapped many overlapping QTL affecting floral divergence, and they likewise concluded that these QTL clusters demonstrate genetic linkage. Hence, our results suggest that floral divergence between *candida* and *collina* subspecies may have resulted from mutations affecting only a few traits (especially flower color) that are correlated with several other characters that follow a hummingbird-hawkmoth pollinator syndrome, followed by pollinator-mediated selection acting on this variation.

A critical component for the evolution of pollination syndromes is that floral display traits (flower color, morphology, and scent, etc.) be accurate signals of the underlying nectar reward (Grant 1949; Baker 1963; Stebbins 1970b; Proctor et al. 1996; Hermann and Kuhlemeier 2011; Knauer and Schiestl 2015). Hence, genes that affect floral display and nectar reward are expected to be genetically correlated in natural populations and will show LD, linkage or pleiotropy, and the corresponding traits will have overlapping/clustering QTL in genetic mapping populations. We did not find this for the large effect QTL for flower color on LG1 as it did not co-localize with a reward trait, such as nectar volume or concentration. However, we did find that the smaller effect flower color locus on LG3 (Col_3_48) co-localized with nectar volume (Vol_3_30). Furthermore, in a typical hummingbird-hawkmoth pollinator syndrome, high volumes of dilute nectar are associated with hummingbird (red) flowers, while low volumes of concentrated nectar are associated with hawkmoth (white) flowers (*e.g.*, Meléndez-Ackerman et al. 1997). Our QTL results corroborate this pattern as *collina* alleles lead to redder flowers and greater nectar volume for these overlapping QTL (Fig. 3, S6). Similarly, all three nectar volume QTL overlap with six floral morphology QTL on LG3, LG5 and LG6, and all but one of these QTL (stigma length, SFL_3_38) have allelic patterns that following a hummingbird-hawkmoth syndrome. The pattern of allelic effects at multiple QTL mostly occurring in the same direction as parental trait differences is consistent with a history of divergent selection (Orr 1998),

although we did not formally test this. Moreover, these results support the roles of both divergent natural selection and genetic correlation in the evolution of different pollination syndromes between *collina* and *candida*.

Anthocyanin biosynthetic pathway gene variation influences both pollinator visitation and flower color

Flower color differences can be generated by coding sequence or gene expression variation in anthocyanin biosynthesis pathway structural genes (Zufall and Rausher 2004). We explored the potential for four structural ABP genes to influence pollinator visitation and flower color in both our QTL analysis and in a large sampling of individuals naturally occurring in the Front Range hybrid zone. Our results strongly implicate *DFR* molecular variation as a significant basis of *collina–candida* divergence. First, the QTL encompassing *DFR* accounted for nearly 36% of the color variation within our mapping population, and overlapped with a HBird visitation QTL and the largest HMoth visitation QTL ($p = 0.52$); *collina* alleles led to greater hummingbird and fewer hawkmoth visitations. Second, enrichment in *DFR* gene expression directly correlated with redder flowers across a large sampling of individuals, even after accounting for strong population structure in flower color. Additionally, mean population flower color covaried with mean *DFR* gene expression across the 15 sampled sites. Third, the SNP variants we found for *DFR* were significantly associated with both gene expression and flower color, where the variant with enriched expression produced redder flowers.

In contrast, our analyses of *CHS, F3H* and *ANS* molecular variation did not yield consistent results connecting these loci to flower color variation, but they could affect *collina-candida* divergence indirectly through genetic linkage with other floral features. For example, *CHS, F3H* and *ANS* gene expression did not correlate with flower color across individuals or populations, and gene expression levels and flower color between SNP variants for *F3H* or *ANS* do not match (there were no differences for *CHS* variants). However, genetic markers for *CHS* and *F3H* overlap with several flower width QTL and hummingbird visitation, suggesting that genetic variation at these loci may indirectly impact pollinator behavior through correlated effects on floral morphology.

Collectively, this study represents one of the first that has mapped co-localizing QTL for both pollinator visitation, and a gene that affects flower color in diverged populations. Hence, this provides both quantitative genetic-based and gene expression evidence that natural variation at *DFR* leads to floral variation that is a target for pollinator-mediated selection between divergent populations in a hybrid zone. Several other studies have documented the importance of *DFR* in flower color transitions and floral evolution (Whittall et al. 2006; Des Marais and Rausher 2008; Hopkins and Rausher 2011; Smith and Rausher 2011), suggesting that *DFR* may be a key gene affecting flower color variation, and pollinator-syndromes, across many taxa.

There are several molecular mechanisms for how ABP structural gene variation can affect flower color that could be hypothesized for the *I. aggregata* system studied here. For example, coding region mutations could directly affect the enzymatic function of ABP genes, and/or genetic variation in transcription factors could affect ABP gene expression, and/or mutations to cis-regulatory elements could also affect ABP expression levels. Given that anthocyanins play critical roles in plant function beyond flower color and pollinator attraction (Holton and Cornish 1995), ABP gene coding region mutations that alter overall enzyme activity are unlikely to be selectively favored due to potentially detrimental pleiotropic effects (Streisfeld and Rausher 2011). Here, our results point towards flower color differences resulting from *DFR* expression level changes—and hence either cis-regulatory or linked transcription factor variation—potentially leading to adaptive divergence between *candida*/*collina*. Altered expression of ABP genes driven by cis-element and/or transcription factor variation has been documented in several species (*e.g.*, Des Marais and Rausher 2010; Hopkins and Rausher 2011), suggesting that this is an important evolutionary mechanism for minimizing the potentially negative effects of pleiotropy. Hence, tissue specific expression of ABP genes—governed by cis-regulation—may enable adjustments in flower color between divergent populations, while maintaining normal ABP function elsewhere in plant tissues. Although not quantified, we observed that leaves and bolting shoots clearly do produce anthocyanin pigments. Future studies that explore ABP gene expression and anthocyanin levels across different tissues in both *collina* and *candida* will be helpful in elucidating the role of tissue-specific gene expression and pleiotropy in generating flower color variation in this system.

Conclusion

In our previous work, we demonstrated significant genetic divergence in the *collina*/*candida* subspecies complex for floral traits that followed a hummingbird-hawkmoth pollination-syndrome. This was a somewhat surprising result given evidence for weak genetic differentiation at neutral markers in the Front Range hybrid zone (Milano et al. 2016). Because we found support for pervasive gene flow across *I. aggregata* populations (Milano et al. 2016), divergent selection would necessarily have to be remarkably strong and coordinated across multiple quantitative phenotypes, to maintain the level of divergence we previously reported. Here we show that floral trait divergence in this region may have resulted from persistent correlated trait evolution driven primarily from pollinator-mediated selection acting on a few large effect polymorphisms, particularly those that govern flower color and are genetically linked to other traits. Hence, our present study suggests that divergent phenotypic selection, genetic correlations, and a relatively simple genetic architecture for flower color may indeed be sufficient to result in significant floral divergence between populations.

MATERIALS AND METHODS

Natural history

Ipomopsis aggregata is a short-lived perennial wildflower distributed across the western US. Subspecies *candida* and *collina* have overlapping ranges, and are found in grassy meadows and disturbed montane habitats on the East Slope in the Front Range of the Colorado Rockies, ranging in elevation from 1740 m to over 3050 m (Wilken and Allard 1986). Following germination, *I. aggregata* remains as a rosette for 2-5 years before producing indeterminate inflorescence stalks, after which it reproduces and dies (*i.e.*, follows a monocarpic life cycle). Inflorescences of *I. aggregata* are showy, with hermaphroditic flowers that are protandrous and self-incompatible. Subspecies *candida* and *collina*, along with their hybrids, produce flowers with a range of colors from white and light shades of pink, to a dark red (Fig. 1A and B). Flowers of *I. aggregata* are visited by a range of pollinators, that primarily include the white-lined hawkmoth (Sphingidae: *Hyles lineata*), broad-tailed Hummingbirds (*Selaphorus platycerus*), Rufous Hummingbirds (*Selaphorus rufus*), and Calliope Hummingbirds (*Stellulla calliope*) (Elam and Linhart 1988).

Crossing design

We used a 4-way outbred crossing design to create a mapping population. First, one-way crosses were performed between grandparents (Cuchara × Wilkerson pass and Spring creek × Lefthand canyon) to make four parents (F_1 generation). The *collina*-like Cuchara and Spring creek plants accepted pollen from the *candida*-like Wilkerson pass and Lefthand canyon plants. Subsequently, two parents (F_1s) from each cross were reciprocally crossed, creating two large outbred full-sib families (F_2 generation; family 1 N = 384, family 2 N = 384, total F_2 N=768; see Fig. 1B and C for crossing design). Thus, each progeny in the mapping population is comprised of a mixture of the four grandparental nuclear genomes, carrying 1 of 8 possible allelic combinations at each locus, and has one of two segregating *collina*-like maternal cytoplasms (Cuchara and Spring creek; Fig. 1C). In the context of outbred mapping, a 4-way design carries several advantages. First, by genotyping each grandparent and parent of our crosses, the phase of each allele can be inferred using the multi-generational patterns of inheritance. And second, because we used four grandparents, we increase the probability of obtaining polymorphic genetic markers, and have potentially sampled double the genetic diversity of traditional QTL studies that use only two parents.

Field experiment setup

In the summer of 2005, seeds were cold stratified on wet sand at ~ 4°C for 8 weeks, after which we potted 192 from each maternal cytoplasmic group from both families (1_Cu, 1_Sc, 2_Cu, and 2_Sc) into individual 250 mL Conetainer pots (Stuewe & Sons), for a total of 768 pots. Pots were filled with equal parts Promix BT, sand, and Turface Athletics MVP, and germinated under a long-day photoperiod (16L/8D; supplemented with HPS-lighting of at least 300 μE) in controlled greenhouse conditions at The University of Texas at Austin. Plants were spatially randomized in the greenhouse, watered as needed, and allowed to grow for several months. During this initial germination and early growth phase, we experienced 6.5% mortality;

12 from 1_Cu, 22 from 1_Sc, 1 from 2_Cu, and 12 from 2_Sc. In May 2006, rosettes were transported to an experimental garden, transplanted into a field in a randomized block design, and watered as needed to facilitate establishment; watering was slowly decreased and eventually halted in the summer of 2006. The entire field was fenced to exclude browsing ungulates. The common garden was located in a meadow ~4 km from Nederland, CO (elevation ~2,500 m; coordinates 39.96142°N, 105.5109°W). The meadow was located approximately mid-latitude, longitude and elevation relative to the natural populations we sampled in this study. Two native *candida* populations were adjacent and visible from the common garden site. Transplants experienced a natural overwintering period from fall of 2006 through spring of 2007, and all experimental plants flowered during the 2007 growing season (a few individuals flowered in 2006, and these were removed from the dataset). Following this transplant phase, we experienced an additional mortality of 12.8%; 32 from 1_Cu, 22 from 1_Sc, 20 from 2_Cu, and 8 from 2_Sc. In total, through germination, transplant, and overwintering combined, we lost 129 plants, which were split nearly equally between cytoplasmic groups (65 Cu and 64 Sc), but disproportionately between family 1 and 2 (88 and 41, respectively; $\chi^2 = 17.12$, $p < 0.0001$), suggesting lower vigor with impacts on transplant and overwintering survivorship within family 1.

Phenotypes measured

Flowering time: We recorded the date that each plant produced its first flower during the second season (2007), and scored flowering time as a ranked day beginning with the first individual that flowered.

Floral morphology: During the experiment, we destructively harvested up to 3 flowers per plant at peak flowering, and measured the following seven morphological floral traits on each, which are illustrated in Fig. 1: corolla tube length, stigma length, sepal length, corolla tube width, corolla tube width at the base, petal lobe length, and pedal lobe width. Most of these traits were strongly positively correlated (Fig. S3A), and a principal components analysis (PROC PRICOMP; SAS v9.4) revealed that the first two axes described over 70% of the variation (Fig. S4A). Hence, based on trait loadings, we collapsed these to two floral descriptors that describe flower size (PC1; PCFsize; 55.6% variation explained) and shape (PC2, PCFshape, 15.6% variation explained) of flowers.

Plant size: Near the end of the growing season, we counted the total number of flowers produced by an individual, measured the height of the tallest inflorescence, counted the number of inflorescence branches, and measured the diameter of the root stock at soil level. We again discovered strong correlations within this group of traits (Fig. S4A), so we used a principle components analysis to collapse these four traits into a single size descriptor that explains a majority of variation in these traits (PC1, PCsize, 52.6% variation explained; Fig. S4B).

Flower color: We harvested 1-2 flowers from all plants that were flowering between the dates of 07-20-2007 and 07-24-2007, and collected reflectance spectra for each flower in the

wavelength range of 190-850 nm at 0.5 nm increments using a UV-Vis spectrometer (Stellar Net Inc.). Pure red flowers have no or low reflectance below 550nm and high reflectance above 600nm whereas white flowers have high reflectance throughout the visible spectrum. As flower color shifts from red to white through the color pink the pattern of visible reflectance has an increasingly large peak at 400-480nm. Therefore, the metric of redness we used was the ratio of reflectance at wavelengths 450nm/650nm. On this scale, more red flowers are 0 while more white flowers are 1. We initially calibrated the spectrometer by setting dark zero on a black background and light zero on a white background. We employed a log transformation to improve normality of our color metric for statistical analyses.

Nectar reward: We scored nectar reward for each plant by sampling nectar production of individual flowers. To avoid evaporation from elongating buds, we first taped them closed the afternoon prior to bloom. After 48 hours, the flower was carefully removed from the plant, and nectar was extracted from the base of the corolla using a capillary tube (Microcaps® from Drummon Scientific). Nectar volume was measured by measuring the length of the drawn nectar within the tube, and converting to volume using the known volume/length ratio of the tube. We quantified nectar concentration using a refractometer (Bellingham and Stanley Ltd., England).

Pollinator visitation: We recorded pollinator visitation by direct observation over a three-week period between 30 July and 21 August 2007. We were primarily interested in hummingbird and hawkmoth pollinators. We observed hummingbirds in the morning, late afternoon, and early evening, and hawkmoths during the evening around dusk. To facilitate hummingbird observations, which were challenging due to the number of hummingbirds visiting at once, we split our field into 4 approximately equal-sized blocks, and recorded visitation in each block for 3 or 4 sessions (1 hour each session for a total of 3 or 4 hours per block). Visitation was recorded as the number of flowers visited to an individual plant. For all but two hawkmoth observation sessions, we observed the entire field at once because there were fewer moths in the field at any given time and we were able to follow the relatively slower-flying moths. We recorded hawkmoth visitation over 8 1-hour sessions, for a total of 6 or 7 hours per block. We relativized flower visitation by the number of observation hours for an individual's block and recorded HBird and HMoth as the log transformation of the number of flowers on each plant that was visited by hummingbirds (or hawkmoths, respectively) per hour of effort.

Fitness: We counted the total number of fruits on each plant as an estimate of lifetime fitness. We then calculated relative fitness by dividing the fruit production of each individual plant by the mean fruit production of all experimental plants. All plants that survived to 2007 produced fruits.

Natural selection and pollinator preferences

Prior to analysis, we standardized all traits, including relative fitness, to a mean of 0 and standard deviation of 1, to facilitate comparisons between the effects of different traits on fitness.

Following this, we obtained standardized Pearson product-moment correlation coefficients (r) between all traits using the *pairs.panels* option the of *psych* package in R (Revelle 2017). Our first two models (MODELs 1 & 2) estimated the effect of all measured phenotypes (flowering, PCFsize, PCFshape, PCsize, color, nectar volume and concentration) on relative fitness, and the effects of pollinator visitation (HBird and HMoth) on relative fitness, using two separate generalized linear models (PROC GLM in SAS). We estimated standardized directional selection gradients which we display as arrows in Fig. 2, quadratic (stabilizing or disruptive) selection as the squared term for each trait (*e.g.*, PCFsize*PCFsize) which were doubled (Stinchcombe et al. 2008) and are shown as shaded boxes, and correlational selection between traits by exploring their cross-products (*e.g.*, PCFsize*PCFshape; Lande and Arnold 1983). To obtain selection gradients, we used the SOLUTION option in PROC GLM to calculate the slope of each trait on fitness. To explore pollinator preferences, we used a third and fourth general linear model (MODELs 3 & 4) estimating the effects of physical phenotypes on visitation by hummingbirds and hawkmoths, respectively. For pollinator visitation models, we included the fixed effect block, to account for the four different blocks being observed at different times and/or dates.

Because several traits (e.g., pollinator visitation) remained strongly non-normal following transformation, we opted to carry out all four models described above on 10,000 bootstrap resampled data sets (PROC SURVEYSELECT in SAS), and report the median slope for each trait as its effect size (obtained using PROC UNIVARIATE in SAS); here, we doubled our estimates of non-linear selection (Stinchcombe et al. 2008). We considered an effect to be significant if the fifth or ninety-fifth percentile was greater than or less than zero, respectively (*i.e.*, we used a one-tailed significance value of alpha = 0.05, overall alpha = 0.10, because we were interested in whether the magnitude of the effect size significantly differed from zero, irrespective of the directionality). Residuals for each model were calculated as $\sqrt{(1 - R^2)}$, where R^2 represents the total proportion of the dependent variable explained by the overall model (Kingsolver and Schemske 1991).

Genotyping, linkage map construction, and map coverage

We genotyped the 4-way F_2 mapping population using a combination of 42 microsatellites and 13 expressed sequence tag single nucleotide polymorphisms, EST-SNPs, for a total of 55 genetic markers (Table S2). Microsatellite development is described in earlier work for this system (Stearns et al. 2008), and EST-SNPs were developed from amplicon sequencing of loci derived from expressed sequence tag EST-libraries. Genomic DNA was extracted from leaf tissue using a modified Cetyltrimethyl Ammonium Bromide (CTAB) extraction. Microsatellites were amplified with fluorescently labeled primers in multiplexed PCR reactions using Qiagen's Multiplex PCR Kit (Qiagen, Inc.). Fluorescently labeled PCR fragments were diluted in HiDi™ Formamide (Applied Biosystems, Inc., ABI) with GeneScan™ 500 ROX™ Size Standard (ABI) and analyzed on an ABI 3730 capillary sequencer at The University of Texas at Austin's DNA Core facility. Microsatellite fragment sizes were scored by eye using the programs Genemapper (ABI) and Genemarker (SoftGenetics). SNPs were genotyped using the

ABI Taqman platform at The University of Texas at Austin's DNA Core facility. Several SNPs used to build our linkage map were targeted to candidate ABP genes of interest (see below). The percentage of individuals genotyped for every marker ranged from 44 – 99%, with values below 50% representing markers that were missing in one of the two families (5 markers in family 1 and 8 markers in family 2). The number of individuals genotyped for every marker can be found in Table S2. We also genotyped the grandparents and parents of the F_2 mapping population, allowing determination of allelic phase.

Of the 55 study markers, 42 were polymorphic within both F_2 families, while the remaining 13 were unique to one of each of the families (five and eight, respectively). It is possible to obtain many different segregation types at each genetic marker for outbred crossing designs, depending on the genotype of the grandparents of the mapping population. As a result, segregation at any given marker in the mapping population could yield a fully informative marker representing four grandparental alleles (*e.g.*, AB×CD), or partially informative markers with 3 or fewer alleles segregating. Of the 42 markers common to both crosses, 26 were fully informative and the remainder were partially informative tri- and/or di-allelic; in several cases a marker was tri-allelic in one family, and di-allelic in the other. Of the 13 markers unique to one of the families, five were fully informative in that family, and the remainder were partially informative. Table S2 provides segregation type for all 55 markers used here.

We first constructed separate linkage maps for each family of F_2 progeny obtained from the two parental crosses, which is typical for outbred mapping populations (Haley et al. 1994). We generated both maps using identical protocols in JoinMap v. 4.1 based on a full-sib family (CP) design and a multi-point maximum likelihood algorithm (Van Ooijen 2006). Genetic markers were first assembled into linkage groups using a conservative logarithmic odds-ratio (LOD) of 5.0; LOD scores of 3.0 or greater yielded 7 linkage groups, which is in agreement with published karyotypic data for *I. aggregata* (Porter et al. 2010). Marker order on linkage groups was determined using a regression algorithm with the following parameters; pairwise recombination frequencies < 0.4, LOD > 3.0, and a Kosambi mapping function to estimate genetic distances between markers. We then merged similar linkage groups from the two families into single linkage groups using the *Combine groups for map integration* option offered in JoinMap, and marker order and distances were re-calculated for combined linkage groups using the same parameters as above. All QTL mapping described below was carried out on this integrated genetic map.

Estimates for the length of each linkage group (LG) and total map length (d) were obtained directly from R/qtl (in centimorgans, cM), and intermarker distances (s) were estimated as total map length divided by the number of markers. We estimated total genome size (L) using two methods: First, to account for chromosome ends beyond the terminal markers, we added $2s$ to each LG distance. Second, we used the method of Chakravarti et al. (1991), which multiplies the length of each LG by the factor $(m + 1)/(m - 1)$ where m is the number of markers on each LG, and assumes markers are randomly distributed. We then calculated four estimates of

the proportion of the total genome covered by the map (map coverage, c), using the following methods: The first and second estimates simply divide the estimated map length obtained from r/qtl by the two total genome size estimates (d/L). The third and fourth methods employ the equation $c = 1 - e^{-2d/L}$, where L represents our two estimates of total genome size above (Fishman et al. 2001).

We recovered seven linkage groups with a mean of 7.9 markers per linkage group, a mean inter-marker distance of 11.6 cM, and a total map distance of 554.5 cM as estimated by R/qtl. Table S2 provides marker information. We estimated total genome size using two methods: Simply adding the mean inter-marker distance to the terminal ends of each LG yielded a size of 716.2 cM, and the method of Chakravarti et al. 1991) revealed a slightly larger genome size estimate of 721.3 cM. Using these two genome sizes, we obtained four similar map coverage estimates: 77.4% and 76.9% by dividing the map distance (554.5 cM) by each estimate of total genome size, respectively, and 78.8% and 78.5% by plugging the two genome size estimates into the equation $c = 1 - e^{-2d/L}$, respectively.

QTL mapping analysis

We performed QTL mapping using R/qtl (Broman et al. 2003) on all 21 traits. We first carried out initial QTL mapping using *scanone* with Haley-Knott regression (*hk*). We used *normal* models for all but pollinator visitation, which exhibited a strongly right-skewed distribution. Following initial exploration using a two-part model (*2part*) in R/qtl, we determined that pollinator visitation was best treated as a binary trait for QTL mapping (0=unobserved visits, 1=observed visits), and analyzed visitation using the *binary* model in R/qtl. For each trait we performed 1000 permutations to determine the genomewide threshold at an alpha = 0.05 level. Preliminary one-way genome scans showed that maternal cytoplasm (Cuchara or Spring creek) and family had additive effects on QTL LOD scores, and family had, in many cases, strong interactive effects (Fig. S5). Thus, we included maternal cytoplasm and family as additive- and family as interactive- covariates in our QTL models. For each trait we began scanning for the single largest QTL using the model:

y ~ QTL + QTL*family + family + cytoplasm + e

where e denotes residual variation. We then built a multiple QTL model by conditioning on the highest initial QTL peak position and iteratively re-scanning for up to 4 additional QTL. Each QTL was forced to include an interaction with family. At each iteration, we optimized the peak QTL positions by fixing the position of all but one QTL and scanning for the maximum QTL position within the context of the multiple QTL model. After identifying the 5 largest QTL, we performed a backwards model selection until all remaining QTL were larger than the permutations threshold. If no QTL were retained following backwards selection, we concluded that we found no QTL for that trait. We then calculated variance explained by the model and each QTL separately by fitting an ANOVA and iteratively dropping one QTL from the model.

Confidence intervals around significant QTL were determined using a 1.5 LOD drop on either side of the peak position of the QTL. We plotted our linkage map and QTL segments in R using the *segmentsOnMap* function from the *qtlTools* (github.com/jtlovell/qtlTools). We estimated the effect of having each genotype at each significant QTL on the trait in question, and plot these as effect plots. We estimated these effects as least-squared means using the *lsmeans4qtl* function from the *qtlTools* package accounting for cytoplasm and family as additive effects, and family as an interactive effect. To facilitate comparisons, we plot families separately, as well as the combined F_2 mapping population.

Analysis of candidate flower color genes

We explored the potential for SNPs in the ABP to be associated with flower color variation across the Front Range hybrid zone. In 2008, we revisited 15 local occurrences identified as study sites in our previous work (see Table S4 for site summaries), including those where the grandparents for our mapping population originated, collected and stored flower bud tissue using Invitrogen™ RNA*later*™ stabilization solution (Thermo Scientific Inc., Waltham, MA, USA), and extracted RNA for gene expression assays using Qiagen RNeasy kits (Hilden, Germany). To score color, we extracted anthocyanin pigments using the same method as Milano et al. 2016), and quantified absorbance at 492 nm (the wavelength for the pelargonidin, the anthocyanin pigment responsible for red coloring in *Ipomopsis*; Harborne and Smith 1978) on a plate reader (Bechman DTX880). We then standardized absorbance readings by dividing the absorbance at 492 nm by the dry biomass of tissue used, and log transformed this to improve normality. For gene expression assays, we used Taqman hybridization based gene expression assays, and standardized reads using the $2^{-\Delta\Delta CT}$ Method (see Livak and Schmittgen 2001 for details) using ACTIN as a control gene for normalization.

We assessed the association between normalized gene expression at four ABP candidate genes—*CHS*, *F3H*, *DFR*, and *ANS* (Fig. S1)—and flower color using a series of generalized linear mixed models (PROC MIXED in SAS). We first evaluated the relative contribution of gene expression at these target genes on flower color across all individuals by setting color as the dependent variable and expression of each gene as the independent variables. One concern in association studies is the possibility of false positive associations due to population structure. Hence, despite evidence for only weak population genetic structure across these sites (Milano et al. 2016), we included site as a random effect to account for the potential effect of population structure. We consider this a conservative approach as color is strongly genetically differentiated (Milano et al. 2016) and controlling for population structure likely reduces true signal in our analyses. This model was of the following form:

$$\text{Flower color} \sim CHS_{expression} + F3H_{expression} + DFR_{expression} + ANS_{expression} + \text{Site} + e$$

To explore for population structure in flower color and gene expression, we first constructed a mixed model with color as the dependent variable, and site as a fixed independent

variable. We then used four separate mixed models (one for each of *CHS*, *F3H*, *DFR*, and *ANS*) to explore if expression of these genes differed between populations. These models took the following form, where y represents flower color or gene expression for each locus:

y ~ Site + e

Next, given that we identified SNP variants for each target gene, we tested if color and expression differed between SNP variants for each gene across all individuals. Similar to above, we set color as the dependent variable, and SNP variants for each gene (*i.e.*, CHS_SNP, F3H_SNP, DFR_SNP, and ANS_SNP) as the independent variables and included site as a random variable. This model was constructed as follows:

Flower color ~ CHS_SNP + F3H_SNP + DFR_SNP + ANS_SNP + Site + e

Finally, we then examined how expression for each gene was affected by SNP variant for that gene, using a separate mixed model for each gene. We included site in all four of the above tests to account for population structure. These models took the following form:

Expression ~ SNP + e

For all of the above models, e denotes residual variation, and where we compared mean values between populations or SNP variants, we conducted pairwise t-tests on least-squared means using Tukey-Kramer adjustments to control for multiple comparisons.

ACKNOWLEDGEMENTS

We thank Heather Hurston Dragna, Tanya Vo, Sandy Boles, and Tierney Wayne for marker development, genotyping, and/or gene expression analyses, and Tom Lambrecht, Katherine Gerber, and Katherine Kaine for help with field work. We are grateful to the Hoyl family for allowing us to conduct this research on their beautiful property in the Front Range. This manuscript was greatly improved from comments by David Des Marais, and two anonymous reviewers. This work was supported by UT startup funds and a National Science Foundation Career Award (DEB-0546316) to T.E.J.

DATA ACCESSIBILITY

EST libraries; https://www.ncbi.nlm.nih.gov/nucest/?term=txid40742%5bOrganism:exp

LITERATURE CITED

Amrad A, Moser M, Mandel T, de Vries M, Schuurink RC, Freitas L, Kuhlemeier C. 2016. Gain and Loss of Floral Scent Production through Changes in Structural Genes during Pollinator-Mediated Speciation. Curr. Biol. 26:3303–3312.

Ashman T-L, Majetic CJ. 2006. Genetic constraints on floral evolution: a review and evaluation of patterns. Heredity (Edinb). [Internet] 96:343–352. Available from: http://www.nature.com/doifinder/10.1038/sj.hdy.6800815

Austen EJ, Rowe L, Stinchcombe JR, Forrest JRK. 2017. Explaining the apparent paradox of persistent selection for early flowering. New Phytol.

Baker HG. 1963. Evolutionary Mechanisms in Pollination Biology. Science (80-.). 139:877–883.

Baker HG, Hurd PD. 1968. Intrafloral ecology. Annu. Rev. Entomol. 13:385–414.

Bradshaw HD, Schemske DW. 2003. Allele substitution at a flower colour locus produces a pollinator shift in monkeyflowers. Nature 426:176–178.

Brock MT, Dechaine JM, Iniguez-Luy FL, Maloof JN, Stinchcombe JR, Weinig C. 2010. Floral genetic architecture: An examination of QTL architecture underlying floral (Co)variation across environments. Genetics 186:1451–1466.

Broman KW, Wu H, Sen Ś, Churchill GA. 2003. R/qtl: QTL mapping in experimental crosses. Bioinformatics 19:889–890.

Campbell DR. 1989. Measurements of Selection in a Hermaphroditic Plant : Variation in Male and Female Pollination Success. Evolution 43:318–334.

Campbell DR. 1991. Effects of Floral Traits on Sequential Components of Fitness in Ipomopsis aggregata. Am. Nat. 137:713–737.

Campbell DR. 1996. Evolution of Floral Traits in a Hermaphroditic Plant : Field Measurements of Heritabilities and Genetic Correlations. Evolution 50:1442–1453.

Campbell DR. 1997. Genetic and Environmental Variation in Life-History Traits of a Monocarpic Perennial : A Decade-Long Field Experiment. Evolution 51:373–382.

Campbell DR. 2003. Natural selection in Ipomopsis hybrid zones: implications for ecological speciation. New Phytol. 161:83–90.

Campbell DR, Waser NM, Melendez-Ackerman EJ. 1997. Analyzing Pollinator-Mediated Selection in a Plant Hybrid Zone : Hummingbird Visitation Patterns on Three Spatial Scales. Am. Nat. 149:295–315.

Chakravarti A, Lasher LK, Reefer JE. 1991. A maximum likelihood method for estimating genome length using genetic linkage data. Genetics 128:175–182.

Conner J. 2002. Genetic mechanisms of floral trait correlations in a natural population. Nature 420:407–410.

Elam DR, Linhart YB. 1988. Pollination and seed production in Ipomopsis aggregata: Differences among and within flower color morphs. Am. J. Bot. 75:1262–1274.

Etterson JR, Shaw RG. 2001. Constraint to adaptive evolution in response to global warming. Science (80-.). 294:151–154.

Fishman L, Beardsley PM, Stathos A, Williams CF, Hill JP. 2015. The genetic architecture of

traits associated with the evolution of self-pollination in Mimulus. New Phytol. 205:907–917.

Fishman L, Kelly AJ, Morgan E, Willis JH. 2001. A genetic map in the Mimulus guttatus species complex reveals transmission ratio distortion due to heterospecific interactions. Genetics 159:1701–1716.

Fishman L, Kelly AJ, Willis JH. 2002. Minor quantitative trait loci underlie floral traits associated with mating system divergence in Mimulus. Evolution 56:2138–2155.

Forkmann G. 1991. Flavonoids as Flower Pigments : The Formation of the Natural Spectrum and its Extension by Genetic Engineering. Plant Breed. 26:1–26.

Freeman RS, Brody AK, Neefus CD. 2003. Flowering phenology and compensation for herbivory in Ipomopsis aggregata. Oecologia 136:394–401.

Fulton M, Hodges SA. 1999. Floral isolation between Aquilegia formosa and Aquilegia pubescens. Proc. R. Soc. B Biol. Sci. 266:2247–2252.

Grant V. 1949. Pollination Systems as Isolating Mechanisms in Angiosperms. Evolution 3:82–97.

Grant V. 1992. Floral Isolation Between Ornithophilous and Sphingophilous Species of Ipomopsis and Aquilegia. Proc. Natl. Acad. Sci. U. S. A. 89:11828–11831.

Grant V, Wilken DH. 1987. Secondary intergradation between Ipomopsis aggregata candita and I. a. collina (Polemoniaceae) in Colorado. Bot. Gaz. 148:372–378.

Haley CS, Knott SA, Elsen JM. 1994. Mapping quantitative trait loci in crosses between outbred lines using least squares. Genetics 136:1195–1207.

Harborne JB, Smith DM. 1978. Correlations between Anthocyanin Chemistry and Pollination Ecology in the Polemoniaceae. Biochem. Syst. Ecol. 6:127–130.

Hermann K, Kuhlemeier C. 2011. The genetic architecture of natural variation in flower morphology. Curr. Opin. Plant Biol. 14:60–65.

Hoballah ME, Gubitz T, Stuurman J, Broger L, Barone M, Mandel T, Dell'Olivo a, Arnold M, Kuhlemeier C. 2007. Single gene-mediated shift in pollinator attraction in Petunia. Plant Cell 19:779–790.

Hodges SA, Whittall JB, Fulton M, Yang JY. 2002. Genetics of floral traits influencing reproductive isolation between Aquilegia formosa and Aquilegia pubescens. Am. Nat. 159:S51–S60.

Holton T, Cornish E. 1995. Genetics and Biochemistry of Anthocyanin Biosynthesis. Plant Cell 7:1071–1083.

Hopkins R, Rausher MD. 2011. Identification of two genes causing reinforcement in the Texas wildflower Phlox drummondii. Nature 469:411–414.

Hopkins R, Rausher MD. 2012. Pollinator-Mediated Selection on Flower Color Allele Drives Reinforcement. Science (80-.). 335:1090–1092.

Juenger T, Purugganan MD, Mackay TFC. 2000. Quantitative trait loci for floral morphology in Arabidopsis thaliana. Genetics 156:1379–1392.

Juenger TE, Bergelson J. 1997. Pollen and Resource Limitation of Compensation to Herbivory in Scarlet Gilia , Ipomopsis aggregata. Ecology 78:1684–1695.

Juenger TE, Bergelson J. 2000. The evolution of compensation to herbivory in scarlet gilia, Ipomopsis aggregata: herbivore-imposed natural selection and the quantitative genetics of tolerance. Evolution 54:764–777.

Juenger TE, Morton TC, Miller RE, Bergelson J. 2005. Scarlet gilia resistance to insect herbivory: The effects of early season browsing, plant apparency, and phytochemistry on patterns of seed fly attack. Evol. Ecol. 19:79–101.

Juenger TE, Perez-Perez JM, Bernal S, Micol JL. 2005. Quantitative trait loci mapping of floral and leaf morphology traits in Arabidopsis thaliana: Evidence for modular genetic architecture. Evol. Dev. 7:259–271.

Kingsolver JG, Schemske DW. 1991. Path analyses of selection. Trends Ecol. Evol. 6:276–280.

Knauer AC, Schiestl FP. 2015. Bees use honest floral signals as indicators of reward when visiting flowers. Ecol. Lett. 18:135–143.

Lande R, Arnold SJ. 1983. The measurement of selection on correlated characters. Evolution 37:1210–1226.

Lin JZ, Ritland K. 1997. Quantitative trait loci differentiating the outbreeding Mimulus guttatus from the inbreeding M. platycalyx. Genetics 146:1115–1121.

Livak KJ, Schmittgen TD. 2001. Analysis of relative gene expression data using real-time quantitative PCR and the 2-deltadeltaCT method. Methods 25:402–408.

Lovell JT, Juenger TE, Michaels SD, Lasky JR, Platt A, James H, Yu X, Easlon HM, Sen S, Mckay JK. 2013. Pleiotropy of FRIGIDA enhances the potential for multivariate adaptation. Proc. R. Soc. B Biol. Sci. 280:20131043.

Macnair MR, Cumbes QJ. 1989. The Genetic Architecture of Interspecific Variation in Mimulus. Genetics 122:211–222.

Des Marais DL, Rausher MD. 2008. Escape from adaptive conflict after duplication in an anthocyanin pathway gene. Nature 454:762–765.

Des Marais DL, Rausher MD. 2010. Parallel evolution at multiple levels in the origin of hummingbird pollinated flowers in Ipomoea. Evolution 64:2044–2054.

Meléndez-Ackerman AE, Campbell DR, Waser NM. 1997. Hummingbird Behavior and Mechanisms of Selection on Flower Color in Ipomopsis. Ecology 78:2532–2541.

Melendez-Ackerman EJ. 1997. Patterns of Color and Nectar Variation Across an Ipomopsis (Polemoniaceae) Hybrid Zone. Am. J. Bot. 84:41–47.

Melendez-Ackerman EJ, Campbell DR. 1998. Adaptive Significance of Flower Color and Inter-Trait Correlations in an Ipomopsis Hybrid Zone. Evolution 52:1293–1303.

Milano ER, Kenney AM, Juenger TE. 2016. Adaptive differentiation in floral traits in the presence of high gene flow in scarlet gilia (Ipomopsis aggregata). Mol. Ecol. 25:5862–5875.

Mitchell-Olds T. 1996. Pleiotropy Causes Long-Term Genetic Constraints on Life-History Evolution in Brassica rapa. Evolution 50:1849–1858.

Mitchell RJ. 1993. Adaptive Significance of Ipomopsis aggregata Nectar Production: Observation and Experiment in the Field. Evolution 47:25–35.

Mitchell RJ. 1994. Effects of floral traits, pollinator visitation, and plant size on Ipomopsis aggregata fruit production. Am. Nat. 143:870–889.

Mitchell RJ, Waser NM. 1992. Adaptive Significance of Ipomopsis Aggregata Nectar Production: Pollination Success of Single Flowers. Ecology 73:633–638.

Nakazato T, Rieseberg LH, Wood TE. 2013. The genetic basis of speciation in the Giliopsis lineage of Ipomopsis (Polemoniaceae). Heredity (Edinb). 111:227–237.

Van Ooijen JW. 2006. JoinMap (R) 4, Software for the calculation of genetic linkage maps in experimental populations.

Orr HA. 1998. Testing natural selection vs. genetic drift in phenotypic evolution using quantitative trait locus data. Genetics 149:2099–2104.

Paulsen S, Rausher MD. 2000. Brief communication: Floral-color polymorphism in Ipomeoea purpurea: biased inheritance of the dark allele is not a general explanation for is maintenance. J. Hered. 91:491–495.

Porter JM, Johnson LA. 2000. A phylogenetic classification of Polemoniaceae. Aliso 19:55–91.

Porter JM, Johnson LA, Wilken D. 2010. Phylogenetic Systematics of Ipomopsis (Polemoniaceae): Relationships and Divergence Times Estimated from Chloroplast and Nuclear DNA Sequences. Syst. Bot. 35:181–200.

Proctor M, Yeo P, Lack A. 1996. The natural history of pollination. Portland: Timber Press

Quattrocchio F, Wing J, van der Woude K, Souer E, de Vetten N, Mol J, Koes R. 1999. Molecular analysis of the anthocyanin2 gene of petunia and its role in the evolution of flower color. Plant Cell 11:1433–1444.

Rausher MD. 2008. Evolutionary Transitions in Floral Color. Int. J. Plant Sci. 169:7–21.

Revelle W. 2017. psych: Procedures for personality and psychological research. Available from: https://cran.r-project.org/package=psych Version=1.7.3

Schemske DW, Bradshaw HD. 1999. Pollinator preference and the evolution of floral traits in monkeyflowers (Mimulus). Proc. Natl. Acad. Sci. U. S. A. 96:11910–11915.

Smith J, Burian R, Kauffman S, Alberch P, Campbell J, Goodwin B, Lande R, Raup D, Wolpert L. 1985. Developmental constraints and evolution. Q. Rev. Biol. 60:265–287.

Smith SD. 2016. Pleiotropy and the evolution of floral integration. New Phytol. 209:80–85.

Smith SD, Rausher MD. 2011. Gene loss and parallel evolution contribute to species difference

in flower color. Mol. Biol. Evol. 28:2799–2810.

Stearns F, Boles S, Hurston H, Vo T, Butler D, Shuham W, Juenger TE. 2008. Identification of nuclear microsatellite loci for Ipomopsis aggregata and the distribution of pairwise relatedness in a natural population. Mol. Ecol. Resour. 8:437–439.

Stebbins GL. 1970a. Adaptive Radiation of Reproductive Characteristics in Angiosperms , I : Pollination Mechanisms. Annu. Rev. Ecol. Syst. 1:307–326.

Stebbins GL. 1970b. Adaptive Radiation of Reproductive Characteristics in Angiosperms, I: Pollination Mechanisms. Annu. Rev. Ecol. Syst. 1:307–326.

Stinchcombe JR, Agrawal AF, Hohenlohe P a, Arnold SJ, Blows MW. 2008. Estimating Nonlinear Selection Gradients Using Quadratic Regression Coefficients : Double or Nothing? Evolution 62:2435–2440.

Streisfeld MA, Rausher MD. 2011. Population genetics, pleiotropy, and the preferential fixation of mutations during adaptive evolution. Evolution (N. Y). 65:629–642.

Subramaniam B, Rausher MD. 2000. Balancing Selection on a Floral Polymorphism. Evolution 54:691–695.

Wessinger CA, Rausher MD. 2015. Ecological transition predictably associated with gene degeneration. Mol. Biol. Evol. 32:347–354.

Whittall JB, Voelckel C, Kliebenstein DJ, Hodges SA. 2006. Convergence, constraint and the role of gene expression during adaptive radiation: Floral anthocyanins in Aquilegia. Mol. Ecol. 15:4645–4657.

Wilken DH, Allard ST. 1986. Intergradation among Populations of the Ipomopsis aggregata Complex in the Colorado Front Range. Syst. Bot. 11:1–13.

Wolf PG, Soltis PS. 1992. Estimates of gene flow among populations, geographic races, and species in the Ipomopsis aggregata complex. Genetics 130:639–647.

Wolf PG, Soltis PS, Soltis DE. 1991. Genetic Relationships and Patterns of Allozymic Divergence in the Ipomopsis aggregata Complex and Related Species (Polemoniaceae). Am. J. Bot. 78:515–526.

Yuan YW, Sagawa JM, Young RC, Christensen BJ, Bradshaw HD. 2013. Genetic dissection of a major anthocyanin QTL contributing to pollinator-mediated reproductive isolation between sister species of Mimulus. Genetics 194:255–263.

Zufall RA, Rausher MD. 2004. Genetic changes associated with floral adaptation restrict future evolutionary potential. Nature 428:847–850.

FIGURE LEGENDS

Figure 1. (A) Images of flowers taken from the grandparental lines used in our cross. Wilkerson pass and Lefthand canyon represent *candida*-like and Cuchara and Spring creek represent *collina*-like *I. aggregata*, respectively. **(B)** Example flowers taken from F_2 progeny from our cross, demonstrating the segregation of many quantitative features (*e.g.* color, length, width). **(C)** The 4-way outbred crossing designed used to generate plants for our field experiment and QTL mapping. Two separate F_1 lines from each grandparental cross were reciprocally crossed (family 1 and 2), such that the maternal cytoplasm from both Cuchara (Cu) and Spring creek (Sc) are represented in each of the two crosses. **(D)** Morphological features of flowers that were measured in the present study.

Figure 2. **(A)** Diagram illustrating standardized selection gradients for phenotypic traits (MODEL 1) and pollinator visitation (MODEL 2); note that traits and visitation were assessed separately. HBird refers to hummingbird visitation and HMoth refers to hawkmoth visitation. Curved lines represent significant correlations. **(B)** Diagram showing the effect of traits on Hummingbird (MODEL 3) and Hawkmoth (MODEL 4) visitation, assessed separately. For both **(A)** and **(B)**, straight lines represent a significant direct effect (solid lines indicate a positive relationship while hatched lines indicate a negative relationship), and shaded boxes represent a non-linear effect on fitness (A) or hummingbird visitation (B) only (see text and Fig. S4 for a summary of curvature). The thickness of all lines represents the magnitude of the effect size. A summary of all linear and non-linear coefficients and model residuals can be found in Table S1. **(C)** Surface plots for predicted visitation generated from MODEL 3 (Hummingbird) and MODEL 4 (Hawkmoth) models. Note that in **(B)** the hatched connecting Color and HBird indicates that redder flowers attract more hummingbird pollinators (see Materials and Methods for a description of our color metric).

Figure 3. *Ipomopsis aggregata* genetic linkage map with marker positions and all identified QTL mapped to the right of its linkage group. The size of the segments represents 1.5 LOD drop confidence intervals, white points represent the peak position of the QTL, and the shape (round or square) and stripes are to help differentiate similarly colored QTL segments. SNP positions for the four ABP genes analyzed in this study are shown as black boxes pointing to the marker that represents that SNP: *CHS*, *chalcone synthase*; *F3H*, *flavanone-3-hydroxylase*; *DFR*, *dihydroflavonol 4-reductase*; *ANS*, *anthocyanidin synthase*.

Figure 4. (A) LOD profiles for the large effect flowering time QTL located on linkage group 7 (FT_7_64), and for the large effect flower color QTL located on LG1 (Col_1_61.2). The hatched lines represent the $\alpha = 0.05$ LOD cutoff for significance estimated from 1,000 permutations, and the ticks above the x-axes represent marker positions. Effect plots showing the least-squared mean (± SE) phenotype of each genotype for **(B)** Hummingbird and **(C)** Hawkmoth visitation

rates to plants with the specified genotype at the flower color QTL on LG1, **(D)** the flowering time QTL on LG7, and **(E)** the flower color QTL on LG1 (*i.e*., *DFR*) with more negative values indicating redder flowers. We estimated lsmean trait values for families separately (Family 1 = blue and Family 2 = red), and for both families combined (Combined F_2 = black). Ca_1 and Ca_2 represent alleles inherited from *candida*-like grandparents (Wilkerson pass or Lefthand canyon), and Co_1 and Co_2 represent alleles inherited from *collina*-like grandparents (Cuchara or Spring creek).

Figure 5. Patterns of gene expression and color variation. **(A)** Relationship between flower color and DFR gene expression for all individuals collected from across the Front Range. **(B)** Population least-squared means (± 1 SE) for color (bars), and gene expression (symbols) for four ABP loci: *CHS*, *chalcone synthase*; *F3H*, *flavanone-3-hydroxylase*; *DFR*, *dihydroflavonol 4-reductase*; *ANS*, *anthocyanidin synthase*. Arrow heads denote the four populations from which grandparents were derived for our 4-way cross. In contrast to the flower color metric used in our selection analyses, in these plots larger, more positive, values for color represent redder flowers. Lower dCt values equal higher gene expression.

Figure 6. Least squared mean (± 1 SE) gene expression (grey bars) and flower color (pink to red bars) for SNP variants of the four ABP genes, where X's and Y's represent different alleles at each gene. Asterisks and bars with different letters (grey bars) or colors (white to red bars) indicate significant pairwise differences at the p = 0.05 level, and NS indicates non-significance (we report statistics in the main text). Note that only pairwise comparisons of SNP variants within each gene are presented, and not comparisons of variants between genes. In contrast to the flower color metric used in our selection analyses, in these plots larger more positive values for color represent redder flowers. Lower dCt values equal higher gene expression. ABP loci: *CHS*, *chalcone synthase*; *F3H*, *flavanone-3-hydroxylase*; *DFR*, *dihydroflavonol 4-reductase*; *ANS*, *anthocyanidin synthase*.

FIGURES

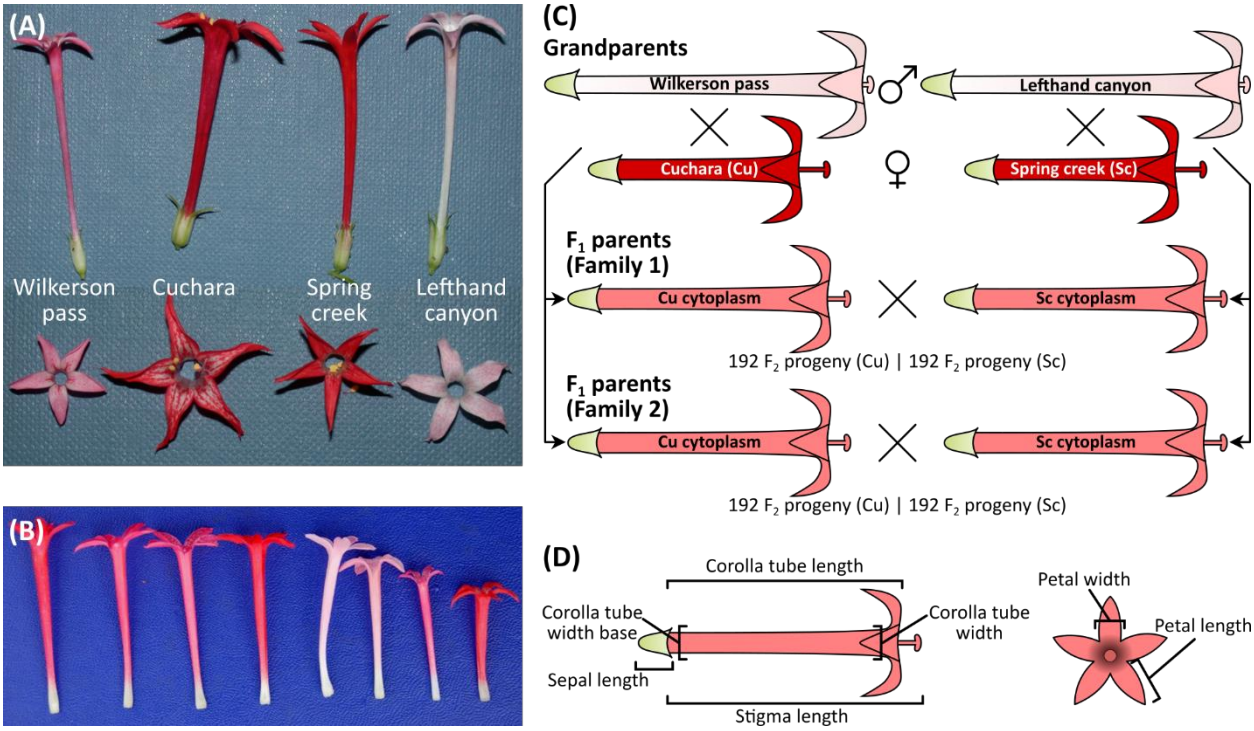

Figure 1. **(A)** Images of flowers taken from the grandparental lines used in our cross. Wilkerson pass and Lefthand canyon represent *candida*-like and Cuchara and Spring creek represent *collina*-like *I. aggregata*, respectively. **(B)** Example flowers taken from F_2 progeny from our cross, demonstrating the segregation of many quantitative features (*e.g.* color, length, width). **(C)** The 4-way outbred crossing designed used to generate plants for our field experiment and QTL mapping. Two separate F_1 lines from each grandparental cross were reciprocally crossed (family 1 and 2), such that the maternal cytoplasm from both Cuchara (Cu) and Spring creek (Sc) are represented in each of the two crosses. **(D)** Morphological features of flowers that were measured in the present study.

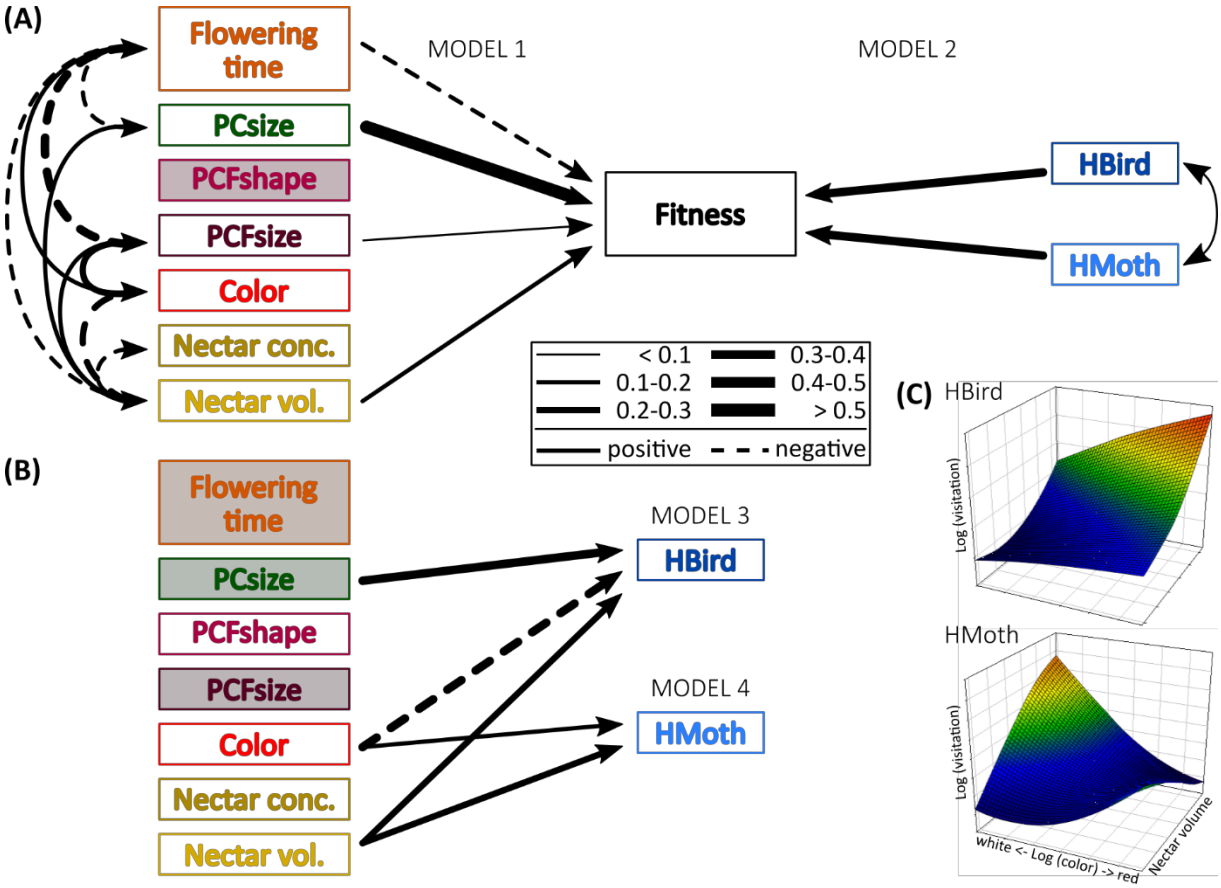

Figure 2. **(A)** Diagram illustrating standardized selection gradients for phenotypic traits (MODEL 1) and pollinator visitation (MODEL 2); note that traits and visitation were assessed separately. HBird refers to hummingbird visitation and HMoth refers to hawkmoth visitation. Curved lines represent significant correlations. **(B)** Diagram showing the effect of traits on Hummingbird (MODEL 3) and Hawkmoth (MODEL 4) visitation, assessed separately. For both **(A)** and **(B)**, straight lines represent a significant direct effect (solid lines indicate a positive relationship while hatched lines indicate a negative relationship), and shaded boxes represent a non-linear effect on fitness (A) or hummingbird visitation (B) only (see text and Fig. S4 for a summary of curvature). The thickness of all lines represents the magnitude of the effect size. A summary of all linear and non-linear coefficients and model residuals can be found in Table S1. **(C)** Surface plots for predicted visitation generated from MODEL 3 (Hummingbird) and MODEL 4 (Hawkmoth) models. Note that in **(B)** the hatched connecting Color and HBird indicates that redder flowers attract more hummingbird pollinators (see Materials and Methods for a description of our color metric).

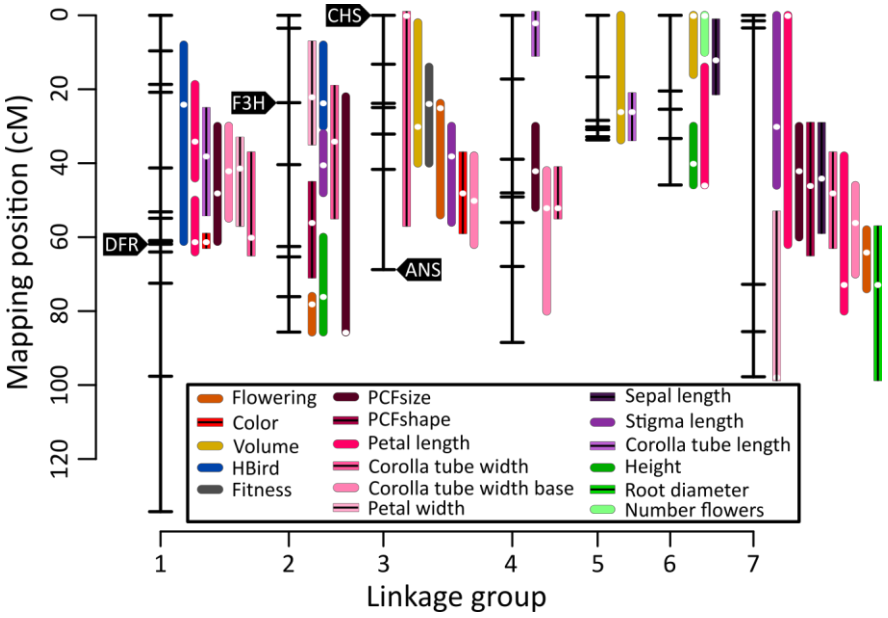

Figure 3. *Ipomopsis aggregata* genetic linkage map with marker positions and all identified QTL mapped to the right of its linkage group. The size of the segments represents 1.5 LOD drop confidence intervals, white points represent the peak position of the QTL, and the shape (round or square) and stripes are to help differentiate similarly colored QTL segments. SNP positions for the four ABP genes analyzed in this study are shown as black boxes pointing to the marker that represents that SNP: *CHS*, *chalcone synthase*; *F3H*, *flavanone-3-hydroxylase*; *DFR*, *dihydroflavonol 4-reductase*; *ANS*, *anthocyanidin synthase*.

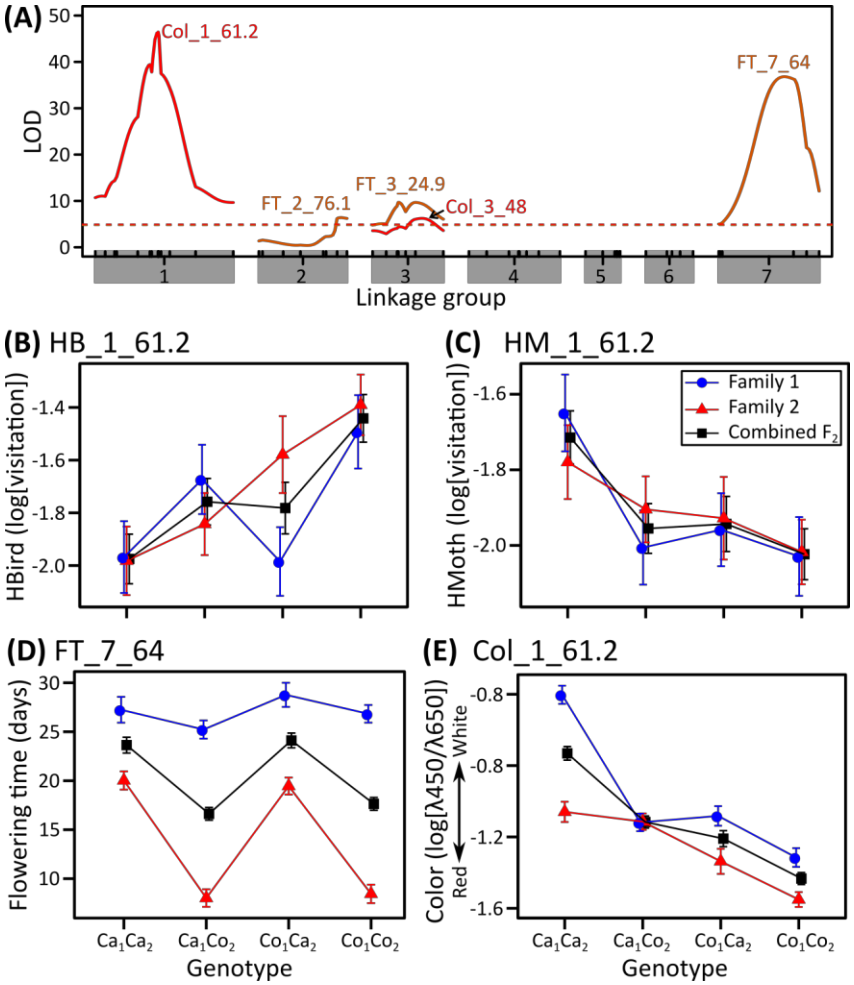

Figure 4. **(A)** LOD profiles for the large effect flowering time QTL located on linkage group 7 (FT_7_64), and for the large effect flower color QTL located on LG1 (Col_1_61.2). The hatched lines represent the α = 0.05 LOD cutoff for significance estimated from 1,000 permutations, and the ticks above the x-axes represent marker positions. Effect plots showing the least-squared mean (± SE) phenotype of each genotype for **(B)** Hummingbird and **(C)** Hawkmoth visitation rates to plants with the specified genotype at the flower color QTL on LG1, **(D)** the flowering time QTL on LG7, and **(E)** the flower color QTL on LG1 (*i.e.*, *DFR*) with more negative values indicating redder flowers. We estimated lsmean trait values for families separately (Family 1 = blue and Family 2 = red), and for both families combined (Combined F_2 = black). Ca_1 and Ca_2 represent alleles inherited from *candida*-like grandparents (Wilkerson pass or Lefthand canyon), and Co_1 and Co_2 represent alleles inherited from *collina*-like grandparents (Cuchara or Spring creek).

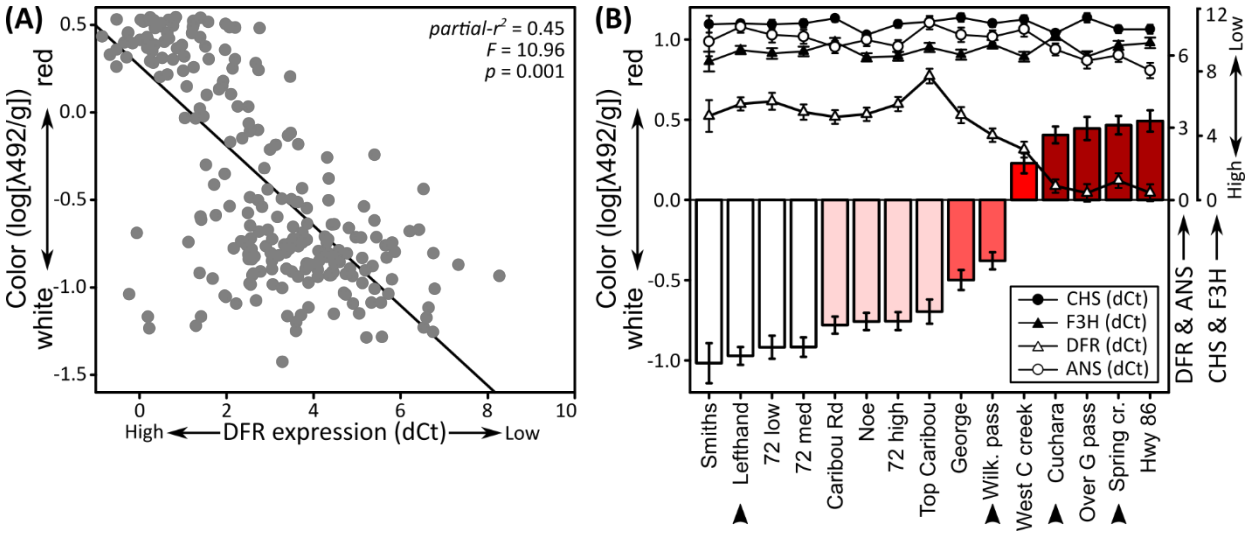

Figure 5. Patterns of gene expression and color variation. **(A)** Relationship between flower color and DFR gene expression for all individuals collected from across the Front Range. **(B)** Population least-squared means (± 1 SE) for color (bars), and gene expression (symbols) for four ABP loci: *CHS*, *chalcone synthase*; *F3H*, *flavanone-3-hydroxylase*; *DFR*, *dihydroflavonol 4-reductase*; *ANS*, *anthocyanidin synthase*. Arrow heads denote the four populations from which grandparents were derived for our 4-way cross. In contrast to the flower color metric used in our selection analyses, in these plots larger, more positive, values for color represent redder flowers. Lower dCt values equal higher gene expression.

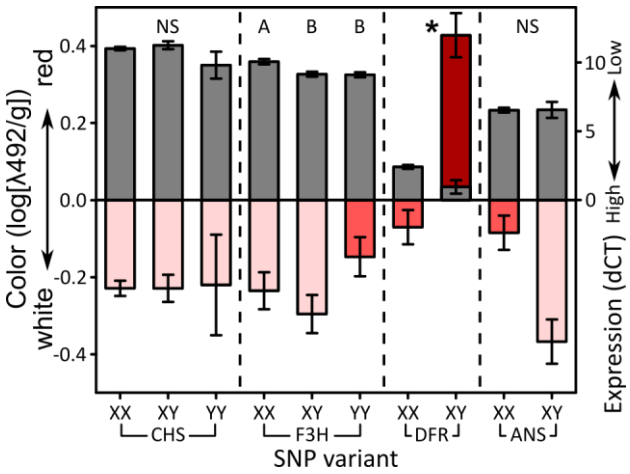

Figure 6. Least squared mean (± 1 SE) gene expression (grey bars) and flower color (pink to red bars) for SNP variants of the four ABP genes, where X's and Y's represent different alleles at each gene. Asterisks and bars with different letters (grey bars) or colors (white to red bars) indicate significant pairwise differences at the p = 0.05 level, and NS indicates non-significance (we report statistics in the main text). Note that only pairwise comparisons of SNP variants within each gene are presented, and not comparisons of variants between genes. In contrast to the flower color metric used in our selection analyses, in these plots larger more positive values for color represent redder flowers. Lower dCt values equal higher gene expression. ABP loci: *CHS*, *chalcone synthase*; *F3H*, *flavanone-3-hydroxylase*; *DFR*, *dihydroflavonol 4-reductase*; *ANS*, *anthocyanidin synthase*.